Journal of Alloys and Compounds 693 (2017) 887–894

Contents lists available at ScienceDirect

Journal of Alloys and Compounds

journal homepage: http://www.elsevier.com/locate/jalcom

A structural and magnetic study of $Nd_5Fe_2B_6$ and $Nd_5Fe_2B_6D_{4.1}$

S. Tencé [a, b, c, d, *], A. Wattiaux [a, b], M. Duttine [a, b], R. Decourt [a, b], O. Isnard [c, d]

[a] CNRS, ICMCB, UPR 9048, F-33600 Pessac, France
[b] Univ. Bordeaux, ICMCB, UPR 9048, F-33600 Pessac, France
[c] Univ. Grenoble Alpes, Inst NEEL, F-38042 Grenoble, France
[d] CNRS, Inst NEEL, F-38042 Grenoble, France

ARTICLE INFO

Article history:
Received 21 July 2016
Received in revised form
30 August 2016
Accepted 22 September 2016
Available online 23 September 2016

Keywords:
Boron hydride
Hydrogenation
Magnetic measurements
^{57}Fe Mössbauer spectroscopy
Neutron diffraction
Magnetic structure

ABSTRACT

We investigated the structural and magnetic properties of the boride $Nd_5Fe_2B_6$ and of the deuteride $Nd_5Fe_2B_6D_{4.1}$ by means of magnetization and specific heat measurements, Mössbauer spectroscopy and neutron powder diffraction. In $Nd_5Fe_2B_6D_{4.1}$, deuterium atoms are located in two inequivalent interstitial sites: one octahedral D1 [Nd6] and one tetrahedral D2 [Nd3Fe], both avoiding B as near neighbor. This insertion induces a pronounced anisotropic unit cell expansion along the *c*-axis. While the $Nd_5Fe_2B_6$ compound exhibits a magnetic ordering below about 68 K, the deuteride exhibits a lower ordering temperature of about 21 K as a consequence of D insertion in the Nd environment. For both compounds powder neutron diffraction investigations have evidenced a ferromagnetic structure with magnetic moments along the *c*-axis. However, in the deuteride, the Nd magnetic moments values are reduced and that of Fe vanishes. ^{57}Fe Mössbauer spectroscopy confirms the existence of a small ordered magnetic moment on iron in $Nd_5Fe_2B_6$ and the presence of two environments for Fe in the deuteride.

1. Introduction

The discovery of the excellent magnetic properties of $Nd_2Fe_{14}B$ for applications as a permanent magnet material with high energy product has motivated the studies of the ternary phase diagrams *R*-Fe-B (*R* = Rare-earth). In this way, new borides of $Pr_{5-x}Co_{2+x}B_6$-type structure containing iron and cobalt have been obtained in 1986 by Dub et al. for *R* = Y, La, Ce, Pr, Nd, Sm, Eu, Gd, Tb, Dy, Ho, Er, Tm, Yb, Lu [1]. The crystal structures of these borides $R_5T_2B_6$ (*T* = transition metal) have been determined previously by X-ray diffraction and the existence of a homogeneity range has been stated for some of them [1,2]. They crystallize in the trigonal space group *R*-3*m* with the unit cell parameters a ≈5.4 Å and c ≈ 23 Å. The structure consists of a stacking of alternated [R_3] and [$R_2T_2B_6$] blocks along the c-axis, yielding $R_5T_2B_6$ as final composition of the stoichiometric boride. The [$R_2T_2B_6$] layer contains a flat net of boron atoms which is surrounded by the iron atoms as nearest neighbors. Thus, the structure possesses 3 different sites for *R*, one for *T* and one for B. The homogeneity range for some compounds comes from the possible substitution of the transition metal for the rare earth on the R1 and R3 sites.

It is possible to synthesize the hydrides $R_5T_2B_6H_x$ from the $R_5T_2B_6$ borides by heating them in hydrogen gas [3–6]. Stable hydrides are formed in rather mild hydrogenation conditions, namely for a temperature up to 200 °C and for a hydrogen pressure of about 1 bar. Much higher temperatures and pressures conditions provoke the disproportionation of the $R_5T_2B_6$ boride. Hydrogen insertion yields an anisotropic volume expansion due to the strong increase of the *c* parameter whereas *a* remains unchanged or decreases slightly. So far the absorption-desorption behaviour of hydrogen in those borides has been widely studied [3–6] but the crystal structure of the hydrides has never been determined precisely. The deuterium atoms can be situated in different interstices in the host structure such as R6, R4, R3T, R2TB or R2B2 interstices. Besides, their magnetic properties have been barely measured since only the diminution of the Curie temperature of $Nd_5Fe_2B_6$ and $Gd_5Fe_2B_6$ upon hydrogen uptake has been reported [3,7]. Indeed, T_C decreases from 67 to 20 K for the Nd compound and from 74 to 47 K for the Gd one whereas the Curie temperature of other ternary *R*-Fe-B boride like $R_2Fe_{14}B$ ferromagnets increases upon hydrogenation [8].

The aim of this work is to study the influence of hydrogenation on the magnetic properties and structure of $Nd_5Fe_2B_6$. For this, we have prepared specific samples of $Nd_5Fe_2B_6$ and $Nd_5Fe_2B_6D_{4.1}$ for

* Corresponding author. CNRS, ICMCB, UPR 9048, F-33600 Pessac, France.
E-mail address: tence@icmcb-bordeaux.cnrs.fr (S. Tencé).

http://dx.doi.org/10.1016/j.jallcom.2016.09.243
0925-8388/

neutron diffraction with isotopic ^{11}B and deuterium to avoid the high absorption of natural boron and the high incoherent scattering of hydrogen. In this paper, we present magnetization and specific heat measurements, ^{57}Fe Mössbauer spectroscopy and neutron powder diffraction which allows us to locate the deuterium atoms and determine the magnetic structure of $Nd_5Fe_2B_6$ and $Nd_5Fe_2B_6D_{4.1}$.

1.1. Experiments

The sample with the nominal composition $Nd_5Fe_2B_6$ was prepared by melting precisely weighted amounts of high purity elements Nd, Fe and B^{11} (99.9%) in an arc melting furnace. Isotopic boron 11 was used in order to avoid the high absorption of the neutron flux by the natural boron ($\sigma_{abs}(B) = 767.0$ b and $\sigma_{abs}(B^{11}) = 0.0055$ b). Melting was performed 4–5 times to ensure a good homogeneity under a purified argon gas atmosphere. The total weight loss during the overall melting process was lower than 0.4 wt%. X-ray powder diffraction on the as-cast sample revealed the presence of the target boride with the minor binary impurity Nd_2B_5. Then, the as-cast ingot was enclosed in an evacuated quartz tube and underwent a heat treatment at 1073 K for 3 weeks. No reaction between the sample and the quartz tube was observed. X-ray powder diffraction (Cu-K_α radiation) after annealing evidences a nearly single phased sample corresponding to $Nd_5Fe_2B_6$.

To prepare the deuteride, $Nd_5Fe_2B_6$ was firstly heated at 200 °C under vacuum to activate the sample and then exposed to a pressure of 10 bars of D_2 during several hours.

Magnetization measurements were performed using a superconducting quantum interference device (SQUID) magnetometer (Quantum Design MPMS-XL) in the temperature range 5–350 K and in fields up to 4.6 T.

Heat capacity was determined with a standard relaxation method with a Quantum Design PPMS device. Sample of approximately 20 mg was glued to the sample holder using Apiezon N-grease. The heat capacity of the sample holder and grease was measured just before the sample was studied.

^{57}Fe Mössbauer spectra were recorded in transmission geometry using a constant acceleration Halder–type spectrometer with a room temperature ^{57}Co source (Rh matrix). The velocity scale was calibrated, at room temperature, using a metal iron foil. The sample holders with polycrystalline absorbers containing about 10 mg/cm^2 of iron were placed into a liquid Helium cryostat in order to collect ^{57}Fe Mössbauer spectra in the temperature range 4.2 K–293 K. Refinement of the Mössbauer hyperfine parameters was performed using homemade programs and the WinNormos® software (Wissenschaftliche Elektronik GmbH).

Neutron diffraction experiments were performed on the high resolution two-axis powder diffractometer D1B at the Institut Laue Langevin using a wavelength of $\lambda = 2.52$ Å. The neutron detector with 1280 cells covers an angular range of 128°. During the neutron diffraction measurements a cylindrical vanadium sample holder of 6 mm inner diameter was used. The FullProf Suite program was used for nuclear and magnetic structure refinements using the Rietveld method [9].

2. Results and discussion

2.1. Structural results

Both $Nd_5Fe_2B_6$ and $Nd_5Fe_2B_6D_x$ samples were measured on D1B at the same temperature to compare their respective crystal structure parameters. The refinement of the crystal structure of $Nd_5Fe_2B_6$ at 100 K confirms the previous studies [1] but with only one Wyckoff position for Fe and, thus, no homogeneity range (Fig. 1 and Table 1). The first investigation of the neutron diffraction pattern of $Nd_5Fe_2B_6D_x$ at 100 K shows that the Bragg peaks can be indexed with the trigonal space group *R*-3*m* (see Fig. 1), meaning that there is no change in the initial rhombohedral symmetry after deuterium insertion. It is noticeable that a small amount (4 wt%) of

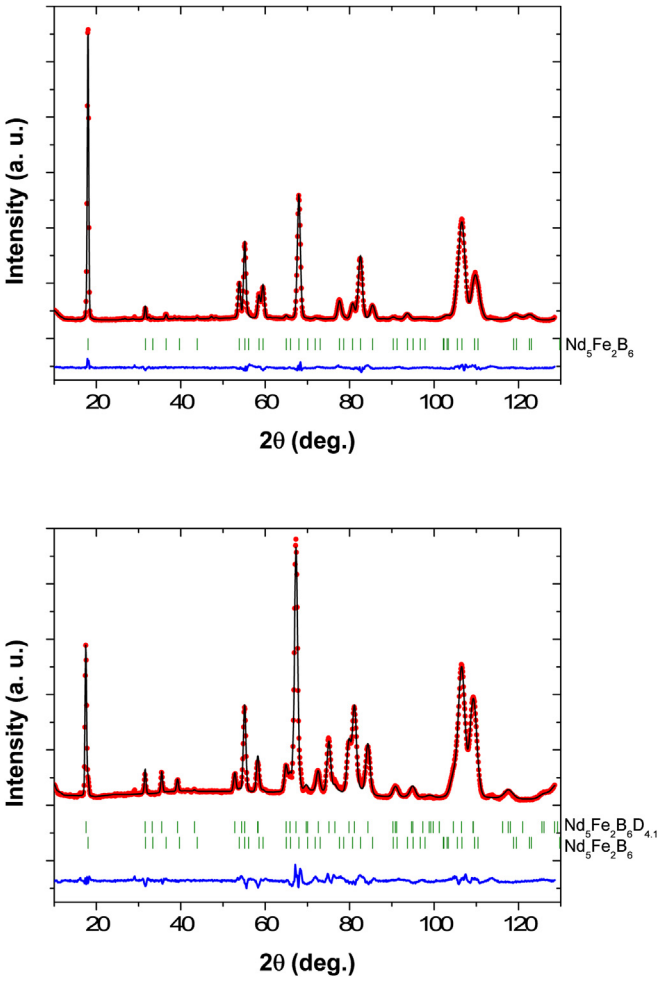

Fig. 1. Refinement of the neutron diffraction pattern of $Nd_5Fe_2B_6$ (up) ($R_B = 4.0\%$, $R_{wp} = 10.7\%$) and $Nd_5Fe_2B_6D_{4.1}$ (down) ($R_B = 3.7\%$, $R_{wp} = 10.7\%$) recorded at 100 K. A small quantity (4 wt%) of the initial boride is still present in the deuterated sample.

Table 1
Crystal structure parameters for $Nd_5Fe_2B_6$ and $Nd_5Fe_2B_6D_{4.1(2)}$ at 100 K. Standard deviation are given in parenthesis.

Position	Wyck.	*x*	*y*	*z*	Occ
Nd1	3*a*	0	0	0	1
Nd2	6*c*	0	0	0.2498 (2)	1
Nd3	6*c*	0	0	0.4181 (2)	1
Fe	6*c*	0	0	0.1171 (2)	1
B	18*g*	0.332	0	0.5	1
a = 5.4430 (4) Å c = 24.133 (3) Å					
Nd1	3*a*	0	0	0	1
Nd2	6*c*	0	0	0.2476 (2)	1
Nd3	6*c*	0	0	0.4178 (2)	1
Fe	6*c*	0	0	0.1170 (1)	1
B	18*g*	0.332	0	0.5	1
D1	9*e*	0.5	0	0	0.85 (1)
D2	36*i*	0.203 (2)	0.026 (4)	0.0664 (6)	0.13 (1)
a = 5.4463 (2) Å c = 24.813 (2) Å					

non deuterated $Nd_5Fe_2B_6$ boride is still present in the sample as indicated in Fig. 1. We observe that the cell parameter *a* does not change much from 5.4430 (4) to 5.4463 (2) Å (+0.06%) whereas *c* strongly increases from 24.133 (3) to 24.813 (2) Å (+2.8%). Therefore, the volume expansion which amounts to +2.9% is strongly anisotropic and mainly along the *c*-axis. This evolution is consistent with that observed by Yartys et al. after hydrogenation of $Nd_5Fe_2B_6$ to obtain $Nd_5Fe_2B_6H_{8.6}$ even if the final H content is not the same [4]. Indeed, they measured at room temperature a unit cell parameters evolution from 5.464 (5) to 5.455 (8) Å (−0.16%) for *a* and from 24.17 (4) to 24.97 (8) Å (+3.3%) for *c*.

In the final refinement, the neodymium, iron and boron atoms were initially put at the same Wyckoff position as in the boride, the (x, y, z) coordinates being then refined in the Rietveld analysis. Among the five main possible interstices it clearly appears that the deuterium atoms are mainly located in the octahedral one [Nd_6] formed by 2 Nd1, 2 Nd2 and 2 Nd3 atoms. This site located in the position D1 (1/2, 0, 0) is filled at 85%. The tetrahedral interstice formed by 3 Nd (Nd1, Nd2 and Nd3) and 1 Fe atoms is also partly occupied by deuterium atoms. This second site [Nd_3Fe] is in the refined position D2 (0.203, 0.026, 0.0664) and is filled at only 13%. The occupancy of these two interstices leads to $Nd_5Fe_2B_6D_{4.1(2)}$ as deuteride formula which is fairly coherent with the mass uptake after deuterium insertion which corresponds to a D content of approximately 4.5 D/f.u. The crystal structure of this deuteride determined from neutron data is depicted in Fig. 2 and the final refinement is shown on Fig. 1. The structural parameters of the boride and the deuteride are gathered in Table 1 and the interatomic distances around Nd, Fe and D atoms are given in Tables 2 and 3. The presence of deuterium atoms in the D1 site implies D1–D1 distances which amount to 2.72 Å. On the other hand the D2 site is only weakly filled since it induces the existence of some too short D2–D2 distances, i.e. 0.82 (x1), 1.25 (x1), 1.80 (x2) and 2.07 Å (x1), this last one being close to the critical distance (2.1 Å) according to the Westlake H–H repulsion criteria [10]. Thus, the D2 site occupancy of 0.13 (1), close to 1/6, is consistent with its deuterium atoms environment. The shortest D-D distance (D1–D2) which is 2.36 Å is comparable to that for $LaNi_3BD_{2.7}$ (2.33 Å) [11] and slightly higher than that in $Nd_2Fe_{14}B$ (2.24 Å) [12].

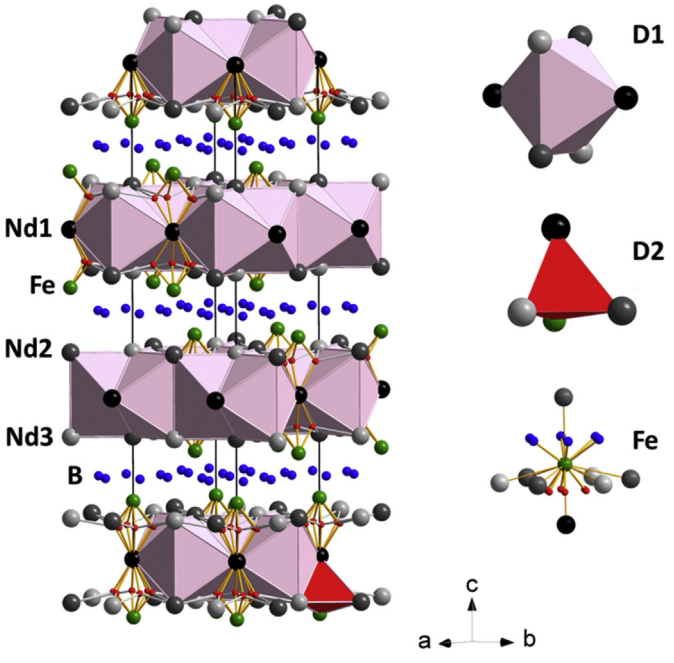

Fig. 2. Left: Crystal structure of $Nd_5Fe_2B_6D_{4.1}$ emphasizing the D2-metal bonds and the network of [Nd_6] octahedra containing deuterium atoms D1. Only one [Nd_3Fe] tetrahedron containing D2 atom is shown for more clarity. Nd, Fe, B and D2 atoms are represented in grayscale, green, blue and red balls, respectively. Right: [Nd_6] octahedron and [Nd_3Fe] tetrahedron containing D1 and D2 atoms, respectively, and coordination of the iron atoms. (For interpretation of the references to colour in this figure legend, the reader is referred to the web version of this article.)

We can argue that the D1 site is initially occupied because it has the most Nd-rich environment and a much larger size compared to D2. One can also assume that the occupancy of the D1 site is maximum before slightly decreasing when the D2 site start to be filled because both sites share a face.

Thus, it appears that deuterium atoms do not have boron as nearest neighbors since none of the [Nd_2FeB] or [Nd_2B_2] interstices in the host structure are filled but only octahedral and tetrahedral interstices essentially formed by Nd atoms. Let's recall that neither elemental iron nor metallic boron absorb a significant amount of hydrogen as described earlier [13] and consequently no hydrogen atom is expected in the close neighborhood of the boron atoms. This observation is in good agreement with earlier reported discussion that B does not accept hydrogen as near neighbor in other Nd-Fe-B ternary intermetallic compounds such as $Nd_2Fe_{14}B$ [12]. In $Nd_2Fe_{14}BH_x$ the H atoms are located firstly in pseudo-tetrahedral sites with three Nd atoms and one Fe and then in sites with two Nd and two Fe atoms as closest neighbors. Our results also confirm those obtained for other borides such $LaNi_3B$ or RT_4B [11,14,15]. For example, in $LaNi_3BD_x$ deuterium atoms have been found in four interstices formed by La and Ni atoms only, i.e. two tetrahedral [La_2Ni_2], trigonal-prismatic [La_3Ni_3] and trigonal-bipyramidal [La_2Ni_3] sites. It confirms the weak interactions between D (or H) and B atoms.

2.2. Magnetization and specific heat measurements

The magnetization measurements performed after zero field cooling (ZFC) and by field cooling (FC) is shown on Fig. 3 for polycrystalline $Nd_5Fe_2B_6$ and the deuteride. The magnetization of the intermetallic (Fig. 3-up) displays a sharp ferro-like transition at 64.5 (5) K (inflection point of M(T)) and a splitting of the ZFC and FC curves since we observe a continuous increase of FC-M(T) below T_C and a pronounced diminution of ZFC-M(T) below 40 K reaching almost zero below 10 K. This behaviour may indicate a strong magnetocrystalline anisotropy or a canted ferromagnetic order. The Curie temperature of the boride, around 68 K, is in fair agreement with all previous results reported on $Nd_5Fe_2B_6$ [16,3].

After deuteration the Curie temperature is significantly reduced to 21 (1) K (Fig. 3-down). The ZFC and FC curves deviate from each other below T_C and also present a second anomaly around 8 K. In the insets of Fig. 3, the inverse of the susceptibility is represented for both samples. For $Nd_5Fe_2B_6D_{4.1}$ the plot clearly shows a Curie-Weiss behaviour and the linear fit leads to a paramagnetic temperature of 9 K and an effective moment of 3.63 μ_B, i.e. the value expected by the Hund's rule for the trivalent state of Nd (3.62 μ_B) which suggests that no magnetic moment is carried by the Fe atom. The inverse of the susceptibility of $Nd_5Fe_2B_6$ exhibits a linear behaviour above 150 K and a Curie-Weiss fit gives an effective moment of 4.2 (1) μ_B which corresponds to $\mu_{eff} = 3.1\ \mu_B$/Fe atom considering $\mu_{eff} = 3.62\ \mu_B$ for Nd^{3+}. This high value of the effective moment suggests that iron is magnetic in this compound. On the other side, the curve for $Nd_5Fe_2B_6$ reveals a gradual decrease of the slope with increasing temperature as can be observed for a ferrimagnetic compound or for a sample with a small amount of an impurity. The fit of the data tacking into account an extra contribution χ_0 (6.10^{-3} mol/emu) in addition of the Curie-Weiss law gives an effective moment of 3.48 μ_B and $\theta_p = 56$ K.

The effective iron magnetic moment found with the Curie-Weiss

Table 2
Interatomic distances around the Nd and the Fe atoms (in Å) for the $Nd_5Fe_2B_6$ and $Nd_5Fe_2B_6D_{4.1(2)}$ compounds.

Distances		$Nd_5Fe_2B_6$	$Nd_5Fe_2B_6D_{4.1}$	Distances		$Nd_5Fe_2B_6$	$Nd_5Fe_2B_6D_{4.1}$
Nd1-	Fe × 2	2.826 (5)	2.903 (3)	**Nd3-**	Nd1 × 3	3.750 (3)	3.779 (3)
	Nd2 × 6	3.734 (3)	3.796 (3)		Nd3 × 1	3.953 (7)	4.079 (7)
	Nd3 × 6	3.750 (3)	3.779 (3)		Nd2 × 1	4.062 (7)	4.223 (7)
	B × 12	4.4124 (5)	4.5164 (3)		B × 6	4.132 (2)	4.165 (2)
Nd2-	B × 6	2.705 (4)	2.7071 (4)				
	Nd3 × 3	3.1427 (2)	3.1446 (1)	**Fe-**	D2 × 6	–	1.63 (2)
	Fe × 1	3.202 (7)	3.239 (1)		B × 6	2.173 (3)	2.194 (2)
	Fe × 3	3.245 (2)	3.241 (6)		Nd1 × 1	2.826 (5)	2.903 (3)
	Nd1 × 3	3.734 (3)	3.796 (3)		Nd2 × 3	3.202 (7)	3.239 (1)
	Nd3 × 1	4.062 (7)	4.223 (7)		Nd2 × 1	3.245 (2)	3.241 (6)
	B × 6	4.146 (2)	4.149 (2)		Nd3 × 3	3.238 (2)	3.246 (2)
Nd3-	B × 6	2.683 (4)	2.731 (4)		B × 6	3.821 (2)	3.834 (1)
	Nd2 × 3	3.1427 (2)	3.1446 (1)		D1 × 6	–	3.980 (2)
	Fe × 3	3.238 (2)	3.246 (1)		Fe × 3	3.950 (4)	3.995 (2)

Table 3
Selected D-D and D-metal distances (in Å) in $Nd_5Fe_2B_6D_{4.1}$.

D1-	D1 × 4	2.7232 (1)	**D1-**	Nd1 × 2	2.7232 (1)
	D2 × 4	2.36 (1)		Nd2 × 2	2.645 (4)
	D2 × 4	2.80 (1)		Nd3 × 2	2.620 (4)
D2-	D2 × 1	0.82 (3)	**D2-**	Nd1 × 1	1.95 (1)
	D2 × 1	1.25 (2)		Nd2 × 1	2.28 (1)
	D2 × 2	1.80 (3)		Nd3 × 1	2.43 (2)
	D2 × 1	2.07 (2)		Fe × 1	1.63 (2)
	D1 × 4	2.36 (2)			
	D1 × 4	2.80 (2)			

fit is large but however smaller than that reported for $ThFe_{11}C_x$ and $R_2Fe_{17}C_x$ type intermetallic compounds [17–19]. Yet, this value is close to the effective magnetic moment of elemental iron, a value of 3.13 μ_B per iron being usually reported for the effective magnetic moment of elemental iron. From the value of $\mu_{eff} = 3.1$ μ_B/Fe atom deduced from the Curie Weiss constant of $Nd_5Fe_2B_6$ we obtain a number of magnetic carrier of 2.26 per Fe atom in the paramagnetic state.

It is worth pointing out that the iron effective magnetic moment deduced from the paramagnetic state is much larger than the Fe magnetic moment obtained in the ordered state (see Section 2.4). Following the Rhodes-Wolfarth plots [20] such behaviour is indicative of the large itinerant character of the Fe magnetism in $Nd_5Fe_2B_6$ compound.

Isothermal magnetization measurements were performed on powder of $Nd_5Fe_2B_6$ at 1.8, 20 and 45 K and on $Nd_5Fe_2B_6D_{4.1}$ at 1.8 and 15 K (Fig. 4). For $Nd_5Fe_2B_6$ the M(μ_0H) virgin curves at 20 and 40 K clearly evidence a ferromagnetic behaviour by a strong rise of M at low fields and a tendency to the saturation at high fields. However, at 1.8 K, the magnetization rises almost linearly at low field then undergoes a sharp increase around 1.5 T and tends to saturate at 7 T. This behaviour may suggest a strong pinning of the domain wall in agreement with the ZFC-M(T). An alternative interpretation could be the occurrence of an antiferro- to ferromagnetic metamagnetic transition. However, this hypothesis is ruled out by the neutron diffraction investigation, as will be presented in Section 2.4, which reveals a ferromagnetic-like ground state. The virgin curves of deuteride clearly suggest a ferromagnetic state but with a lower magnetization at low temperature than the parent boride, namely 10 μ_B/f.u. against 10.8 μ_B/f.u. for $Nd_5Fe_2B_6$. In a nutshell, the hydrogenation of $Nd_5Fe_2B_6$ induces a decrease of the Curie temperature and of the magnetic moment of the Nd atoms.

For further physical characterization we performed specific heat measurements at zero fields which are shown on Fig. 5. The $C_p(T)$

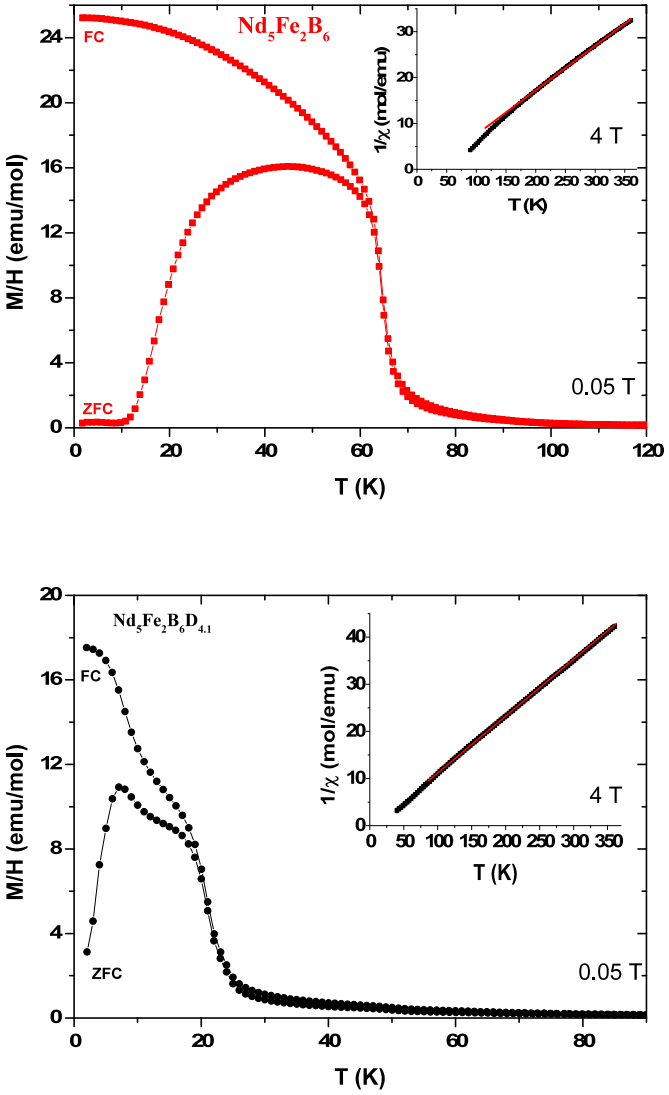

Fig. 3. Thermomagnetic measurements of $Nd_5Fe_2B_6$ (up) and $Nd_5Fe_2B_6D_{4.1}$ (down) collected in zero-field-cooled (ZFC) and field-cooled (FC) modes. The insets present the inverse of the susceptibility *vs* temperature in the paramagnetic regime at $\mu_0H = 4$ T with the Curie-Weiss fit.

curve of the boride exhibits a lambda peak at 64 K, in agreement with the magnetization data. On the other hand the curve of the deuteride presents a less pronounced peak at 21 K and an

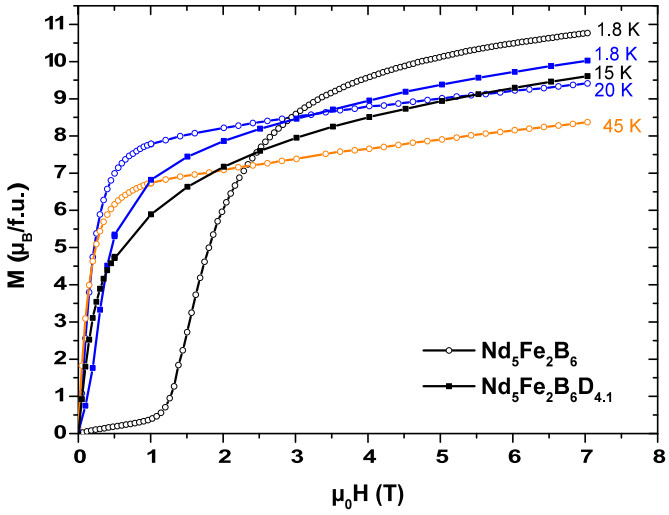

Fig. 4. Field dependence of the magnetization of $Nd_5Fe_2B_6$ (open symbols) and $Nd_5Fe_2B_6D_{4.1}$ (close symbols) for several temperatures.

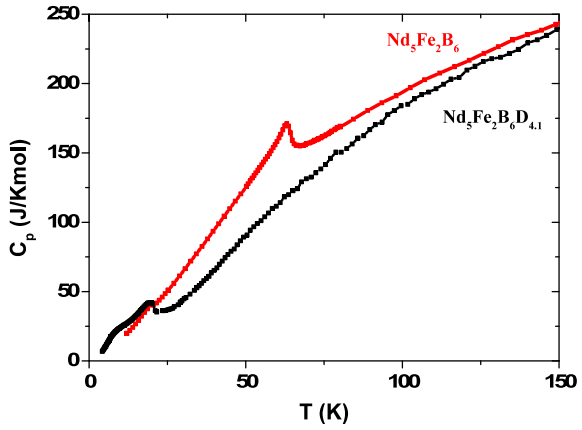

Fig. 5. Specific heat measurements performed on $Nd_5Fe_2B_6$ and $Nd_5Fe_2B_6D_{4.1}$.

additional small bump around 8 K which may corresponds to the second anomaly observed in the magnetization curves.

2.3. Mössbauer spectroscopy

^{57}Fe Mössbauer spectra of $Nd_5Fe_2B_6$ and $Nd_5Fe_2B_6D_{4.1}$ were recorded at room temperature (RT) and 4.2 K (Fig. 6). All the refined hyperfine parameters are gathered in Table 4.

At room temperature the spectrum of the boride can be described by a single quadrupole doublet characteristic of one crystallographic site for the Fe atoms in the structure, in good agreement with the structural results. Indeed, the Mössbauer spectrum was reconstructed considering an asymmetry of the electric field gradient (EFG) and using the full Hamiltonian method (excited-state spin $I = 3/2$ and ground-state spin $I = 1/2$), which led to a good fit of the experimental data. At 4.2 K, in addition to the EFG the iron nucleus also experienced a weak magnetic field which may be transferred from Nd to Fe atoms. The calculated octuplet is then characterized by a non-zero value of the EFG asymmetry parameter ($\eta = 0.6$) and a weak magnetic hyperfine field ($B_{hf} = 2.4$ T). Furthermore, Mössbauer spectra of the $Nd_5Fe_2B_6$ compound were recorded at various temperature from 293 K down to 4.2 K (Fig. 7a) and allowed us to follow the variation with temperature of all hyperfine parameters. As the temperature decreases, the isomer shift increases due to the second-order Doppler effect and the quadrupole splitting (and asymmetry parameter) remains constant (Fig. 7b), which confirms that there is only one crystallographic site for Fe. Moreover, the variation of the hyperfine magnetic field with temperature clearly shows that a magnetic ordering occurs between 72.5 K and 75 K (Fig. 7b). These results are consistent with the magnetic susceptibility measurements as well as the neutron diffraction refinements that did not reveal any structural transition at low temperature but show the presence of a small magnetic moment on the Fe site (see Section 2.4). All these results corroborate and complete the study of Deppe et al. that suggested that an Nd–Fe exchange induced polarization of conduction electrons might give rise to a hyperfine field at the Fe site [21].

The deuteride sample, $Nd_5Fe_2B_6D_{4.1}$, exhibits a quite different Mössbauer signature, revealing that the insertion of deuterium into the boride structure is effective and clearly affects the iron site. At room temperature, the Mössbauer spectrum (Fig. 6) may be considered as the sum of two quadrupole doublets associated with two different local environments for the Fe atoms. The main component (Fe2, about 75%) with a low value of the quadrupole splitting (0.11 mm/s at RT) can be related to Fe atoms located at a crystallographic site with low distortion and with deuterium atoms in its vicinity. The deuteration of the boride $Nd_5Fe_2B_6D_{4.1}$ seems to induce some local constraints that have a direct effect on the symmetry of the Fe sites. The second component (Fe1) of the Mössbauer spectrum is associated with a "non-deuterated" site very similar to the Fe site of the starting boride. The Fe1 signal may actually be analysed as the sum of quadrupole doublets with lorentzian shape (linewidth: 0.30 mm/s), same isomer shift (0.14 mm/s at RT) but different quadrupole splitting values. Such distribution of the quadrupole splitting values (see insets in Fig. 6) as well as the Fe2 signal linewidth (>0.35 mm/s) reflects slight variations of the EFG at the Fe sites due to some local disorder or heterogeneity in site distortion, what could be related to the distribution of deuterium in the D2 [Nd_3Fe] (13%) and D1 [Nd_6] (85%) sites. At 4.2 K, some changes are observed on the Mössbauer spectrum of $Nd_5Fe_2B_6D_{4.1}$ but no magnetic component appears and the relative proportion of the Fe1 and Fe2 components is kept. This suggests that no magnetic field is present on the Fe site, which is in agreement with the magnetic measurement in the paramagnetic regime showing only an effective moment resulting from the trivalent Nd and with the neutron diffraction refinement at 1.8 K.

2.4. Magnetic structure

Several neutron diffraction patterns were recorded from the Curie temperature and down to 1.8 K for both compounds.

In both compounds, magnetic intensities appear below T_C on the nuclear peaks which indicates that the propagation vector is equal to $\mathbf{k} = (0\ 0\ 0)$ and that the magnetic cell corresponds to the nuclear unit cell. Also, the intensities of (0 0 l) lines are null, suggesting that the direction of the magnetic moments is mainly along the *c*-axis since only the magnetic moment component perpendicular to the scattering vector contributes to the magnetic intensity. For $Nd_5Fe_2B_6$ the best refinement is indeed obtained with a ferromagnetic structure with moments parallel to *c* (Fig. 8). The values of the magnetic moments amount to $\mu_1 = 2.36\ (8)\ \mu_B$, $\mu_2 = 2.71\ (6)\ \mu_B$, $\mu_3 = 2.87\ (5)\ \mu_B$ for Nd1, Nd2 and Nd3 respectively and a small moment of 0.8 (2) μ_B is found on the Fe site. Note that our attempts to refine the magnetic structure without contribution of the Fe site, with a canted ferromagnetic structure for example, yielded less good refinements with significant higher agreement factors. Likewise, the same ferromagnetic structure was found for the deuteride

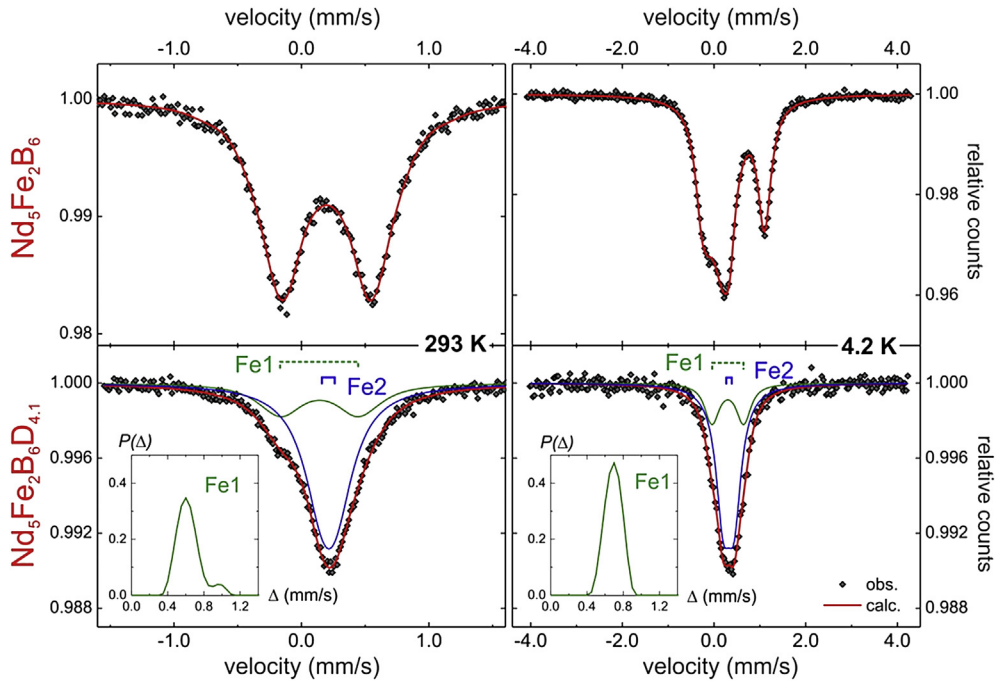

Fig. 6. ^{57}Fe Mössbauer spectra of $Nd_5Fe_2B_6$ and $Nd_5Fe_2B_6D_{4.1}$ recorded at room temperature (left) and 4.2 K (right). Insets: distributions of the quadrupole splitting.

Table 4
^{57}Fe Mössbauer hyperfine parameters for the $Nd_5Fe_2B_6$ and $Nd_5Fe_2B_6D_{4.1}$ compounds. δ: isomer shift, Δ: quadrupole splitting, η: asymmetry parameter of the EFG $\eta \equiv (V_{xx} - V_{yy})/V_{zz}$, B_{hf}: hyperfine magnetic field, Γ: Lorentzian linewidth. *mean value of quadrupole splitting distribution.

		δ (mm/s)	Δ (mm/s)	η	B_{hf} (T)	Γ (mm/s)	Rel. area (%)
$Nd_5Fe_2B_6$							
293 K		0.20 (1)	0.70 (2)	0.6 (1)	–	0.43 (2)	100
4.2 K		0.35 (1)	0.74 (3)	0.6 (1)	2.4 (1)	0.33 (2)	100
$Nd_5Fe_2B_6D_{4.1}$							
293 K	Fe1	0.14 (1)	0.64*	–	–	0.30 (–)	27 (2)
	Fe2	0.22 (1)	0.11 (2)	–	–	0.36 (2)	73 (2)
4.2 K	Fe1	0.30 (2)	0.69*	–	–	0.30 (–)	25 (3)
	Fe2	0.38 (3)	0.24 (5)	–	–	0.34 (2)	75 (3)

except that no significant magnetic moment was found on the Fe atom (Fig. 9). Also, the magnetic moments values are weaker for $Nd_5Fe_2B_6D_{4.1}$ since they are refined to $\mu_1 = 1.92\ (8)\ \mu_B$, $\mu_2 = 1.47\ (5)\ \mu_B$, $\mu_3 = 1.56\ (5)\ \mu_B$ for Nd1, Nd2 and Nd3 respectively. The thermal evolution of the magnetic moments is shown on Fig. 10 for both compounds. Concerning the deuteride, no clear change in the magnetic structure, such as spin reorientation for example, is visible around 8 K as suggested by the thermomagnetic measurement. However, whereas μ_2 and μ_3 increase normally in the whole temperature range, Nd1 tends to saturate rapidly below T_C and to increase again below 10 K. This could explain the second small anomaly observed on the ZFC-FC curve around 8 K. For $Nd_5Fe_2B_6$, $\mu 1$ also saturates rapidly below T_C but the value stays almost constant when decreasing temperature down to 1.8 K contrary to μ_2 and μ_3 which continue to increase. Eventually, $\mu 1$ is significantly higher than μ_2 and μ_3 in the deuteride and inversely in the non-deuterated compound, meaning that $\mu 1$ is much less reduced than μ_2 and μ_3 with hydrogen uptake. This may be related to distance d (D1–Nd1) = 2.72 Å which is much larger than d (D1–Nd2) = 2.64 Å and d (D1–Nd3) = 2.62 Å, so that the magnetic moment of Nd1 is less hampered by the presence of the deuterium in its neighborhood.

The magnetic moment of iron atoms is known to be very sensitive to its local atomic environment, in particular to the presence of metalloid as next near neighbor [22]. The proximity of B atoms in the $Nd_5Fe_2B_6$ crystal structure is clear from the interatomic distances listed in Table 2. According to the considerations discussed in details elsewhere [22] one can expect a rather low magnetic moment on the Fe atoms in $Nd_5Fe_2B_6$. This is indeed what is observed since value of 0.8 μ_B is derived from neutron diffraction results. In the $Nd_5Fe_2B_6$ crystal structure, the Fe atoms neighborhood is both Nd and B rich. Altogether such local atomic environment favors a reduction of the Fe magnetic moment due to electronic hybridization with the Fe 3d orbitals. This effect has been observed in different R-Fe-B ternary compounds for instance, in $Nd_2Fe_{14}B$ the Fe atoms have at most two B as near neighbors [12]. In the $RFe_{4-x}Co_xB$ type compounds the boron richest Fe environment also present only two B near neighbors [23] leading to reduced Fe magnetic moment of about 1.2 μ_B. This effect is expected to be significantly stronger for $Nd_5Fe_2B_6$ compound since its peculiar crystal structure exhibits a large number of Fe near neighbors: 6 B atoms with d (Fe–B) = 2.17 Å. In addition, a calculation of the Wigner-Seitz atomic cell [24] around the Fe position give a moderate value of 11.6 Å^3 assuming the following radii 1.82, 1.26 and 0.92 Å for Nd, Fe and B respectively. As discussed elsewhere, such reduced value does not favor large Fe magnetic moment either [22].

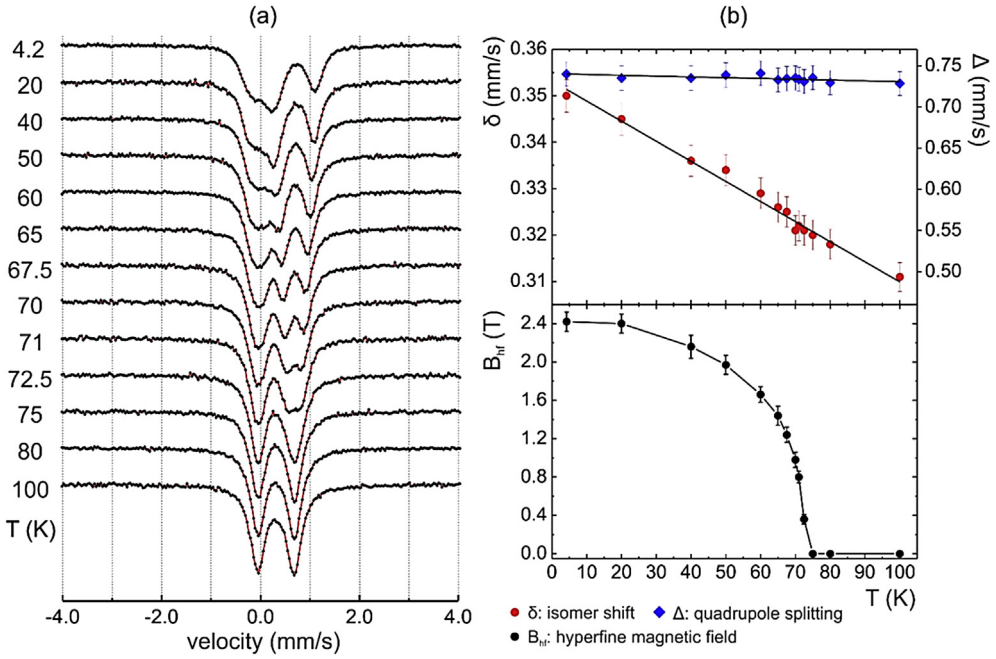

Fig. 7. (a) ^{57}Fe Mössbauer spectra of $Nd_5Fe_2B_6$ recorded at various temperature from 100 K down to 4.2 K. (b) Variation of the refined hyperfine parameters with temperature (solid lines are only guides to the eye).

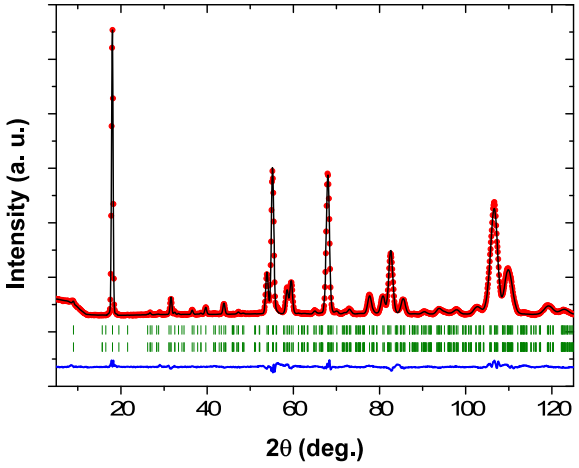

Fig. 8. Neutron diffraction refinement of $Nd_5Fe_2B_6$ at 1.8 K ($R_{B\text{-}nucl}$ = 4.3%, $R_{B\text{-}mag}$ = 3.5%, R_{wp} = 7.0%). The first and the second line ticks correspond to the nuclear and the magnetic Bragg positions respectively.

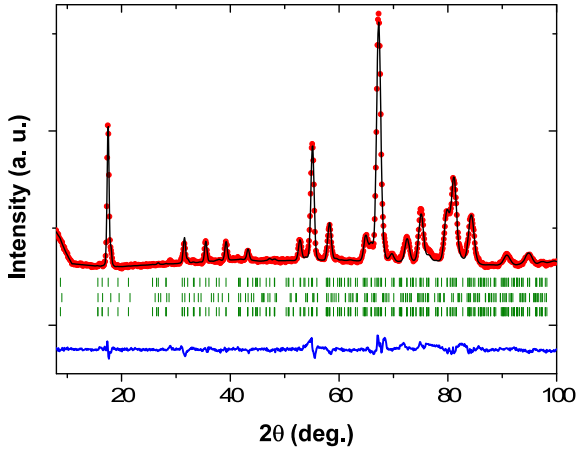

Fig. 9. Neutron diffraction refinement of $Nd_5Fe_2B_6D_{4.1}$ at 1.8 K ($R_{B\text{-}nucl}$ = 5.0%, $R_{B\text{-}mag}$ = 13.5%, R_{wp} = 9.8%). The first and the third line ticks correspond to the nuclear and the magnetic Bragg positions respectively of the deuteride. The second line corresponds to the nuclear peaks of the initial boride.

It is worth to point out that Fe is found to order at the same temperature as the Nd sublattice, which is a remarkably low magnetic ordering temperature for Fe containing intermetallic compound. The fact that the Fe sublattice does not order independently or at least at higher temperature is indicative of the low Fe–Fe exchange interactions. This can be understood in the light of the crystal structure which does not present direct Fe–Fe bonds. The closest Fe–Fe interatomic distances are at 3.95 Å that is much larger than the sum of the metallic Fe radii (2 × 1.27 Å). Such large Fe–Fe interatomic distances most probably preclude the independent magnetic ordering of the iron sublattice. On the contrary the short Nd–Nd interatomic distances are expected to play a crucial role in the establishment of the magnetic ordering, an ordering that is transferred to the Fe atoms via direct and strong Nd–Fe bonds as witnessed by the short Nd–Fe interatomic distances observed in the $Nd_5Fe_2B_6$ compound. Consequently $Nd_5Fe_2B_6$ exhibits an unusual feature: unlike other *R*-Fe binary or ternary intermetallic compounds whose ordering temperature is dominated by Fe–Fe exchange interactions (direct 3d-3d one), the Curie temperature of $Nd_5Fe_2B_6$ compound is dominated by indirect Nd–Nd (of RKKY type) as well as indirect Nd–Fe between the 4f inner shell of Nd and the 3d of Fe mediated by the 5d electrons.

It appears that deuteration of $Nd_5Fe_2B_6$ prevents a magnetic moment from being induced on the Fe atom or it is too small to be measured with neutron diffraction data. This can be accounted for by the diminution of the magnetic moment carried by the neodymium atoms and the increase of the Nd–Fe distances, especially the shortest one Nd1–Fe. Those results are in fair agreement with the magnetic measurement. Last but not least the presence of many D atoms inserted in the local Fe environment maybe detrimental

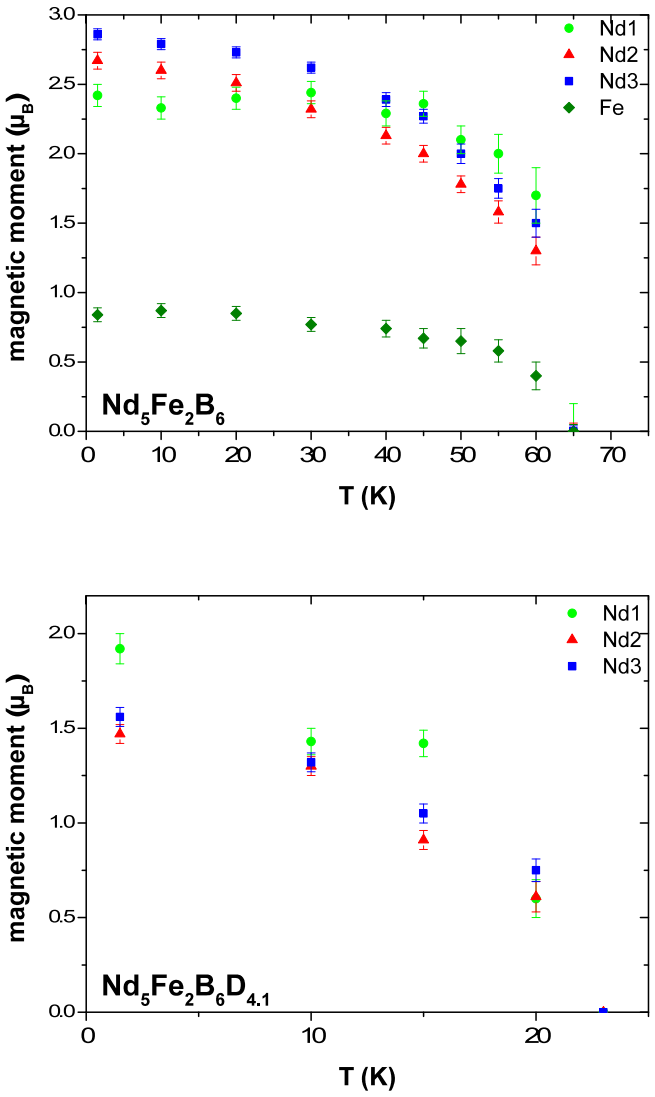

Fig. 10. Thermal evolution of the magnetic moments for $Nd_5Fe_2B_6$ and $Nd_5Fe_2B_6D_{4.1}$ as determined from neutron diffraction data.

for the Fe magnetic moment as it has been reported for YFe_2D_x compounds [25,26]. It was shown by both experimental studies and theoretical calculations that there is no magnetic order for the YFe_2H_5 hydride. In $Nd_5Fe_2B_6$ this occurs via the filling of the D2 position that is the closest to the Fe site.

3. Conclusion

In this paper, the structural and the magnetic properties of the $Nd_5Fe_2B_6$ and $Nd_5Fe_2B_6D_{4.1}$ compounds have been studied by means of magnetization measurements, specific heat, Mössbauer spectroscopy and neutron diffraction, in order to highlight the influence of H/D insertion in the boride on the magnetic behaviour.

The $Nd_5Fe_2B_6$ compound exhibits a magnetic ordering below about 68 K. Powder neutron diffraction investigations have evidenced a ferromagnetic structure with Nd and Fe magnetic moments along the *c*-axis. Complementary ^{57}Fe Mössbauer spectroscopy has been undertaken confirming the existence of a small ordered magnetic moment on iron. The thermal dependence of the hyperfine parameters has been reported between 4.2 and 100 K. The Curie temperature corresponds to a remarkably low magnetic ordering temperature for Fe containing intermetallic compound. Both Fe and Nd atoms are found to carry a magnetic moment and Fe atom is found to order at the same time as the Nd sublattice. This may originate from the low magnetic moment carried by the Fe atoms in the ordered state as well as the non direct Fe–Fe exchange interactions due to long Fe–Fe interatomic distances thus hampering the ordering of the Fe sublattice independently from the Nd one. Indeed a value of about 0.8 μ_B/Fe has been determined from the neutron diffraction investigation a value much smaller than the 2.2 μ_B typical of elemental iron. Such low magnetic moment on the Fe atoms has been attributed to the proximity of boron and the large rare-earth content in the $Nd_5Fe_2B_6$ compound. Analyzing the magnetic properties in both the paramagnetic and ordered state in the frame of the Rhodes-Wolfarth model reveals that in $Nd_5Fe_2B_6$ the Fe 3d magnetism is significantly more delocalized when compared to alpha-Fe.

According to magnetic measurements, specific heat and neutron diffraction investigation, the $Nd_5Fe_2B_6D_{4.1}$ deuteride exhibits a much lower ordering temperature of about 21 K as a consequence of D insertion in the Nd environment. D atoms are accommodated in two inequivalent interstitial sites: one pseudo octahedral D1 [Nd6] and one pseudo tetrahedral D2 [Nd3Fe], both avoiding B as near neighbor. This insertion induces a pronounced anisotropic unit cell expansion along the *c*-axis. The magnetic structure remains ferromagnetic with magnetic moments parallel to the *c*-axis but with reduced values compared to those of the initial boride. Deuterium/hydrogen insertion leads to the destruction of the Fe magnetic moment, which vanishes in the $Nd_5Fe_2B_6D_{4.1}$ compound as evidenced by neutron diffraction experiments and Mössbauer spectroscopy. This most probably arises from electronic effect of D insertion that contributes to partial filling of the 3d electronic band together with the presence of several Nd atoms as near neighbors. Further electronic calculation would be interesting to validate this interpretation.

References

[1] O.M. Dub, N.F. Chaban, Y.B. Kuz'ma, J. Less-Common Met. 117 (1986) 297.
[2] S.O. Yuryev, S.I. Yushchuk, Y.B. Kuz'ma, I.E. Lopatsynsky, J. Alloys Compd. 270 (1998) 16.
[3] V.A. Yartys, A.I. Shtogrin, M.I. Bartashevich, Koord. Khim. 18 (4) (1992) 436.
[4] V.A. Yartys, G. Wiesinger, I.R. Harris, J. Alloys Compd. 252 (1997) 201.
[5] V.A. Yartys, O. Gutfleisch, I.R. Harris, J. Alloys Compd. 253 (1997) 134.
[6] V.A. Yartys, R.V. Denys, O. Gutfleisch, I.I. Bulyk, Y.B. Kuz'ma, I.R. Harris, Int. J. Hydrogen Energy 24 (1999) 189.
[7] V.V. Panasyuk, V.A. Yartys, Z. Phys. Chem. 179 (1993) 479.
[8] P. Dalmas De Reotier, D. Fruchart, P. Wolfers, P. Vulliet, A. Yaouanc, R. Fruchart, P. L'heritier, Journal de Physique Colloques 46 (C6) (1985) C6–C249.
[9] J. Rodriguez-Carvajal, Phys. B 192 (1993) 55.
[10] D.G. Westlake, J. Less-Common Met. 75 (1980) 177.
[11] Y.E. Filinchuk, K. Yvon, Inorg. Chem. 44 (2005) 4398.
[12] O. Isnard, W.B. Yelon, S. Miraglia, D. Fruchart, J. Appl. Phys. 78 (1995) 1892.
[13] S. Rundquist, R. Tellgreen, Y. Andersson, J. Less-Common Met. 101 (1984) 145–168.
[14] F.E. Spada, H. Oesterreicher, R.C. Bowman, M.P. Guse, Phys. Rev. B 30 (1984) 4909–4924.
[15] F. Spada, H. Oesterreicher, J. Less-Common Met. 90 (1983) L1–L4.
[16] K.H.J. Buschow, D.B. De Mooij, J.L.C. Daams, H.M. Van Noort, J. Less-Common Met. 115 (1986) 357.
[17] O. Isnard, V. Pop, K.H.J. Buschow, J. Magn. Magn. Mat. 256 (2003) 133.
[18] E. Burzo, F. Givord, C. R. Acad. Sci. Paris 271 (1970) 1159–1161.
[19] O. Isnard, V. Pop, K.H.J. Buschow, J. Appl. Phys. 101 (2007), 103908–103908.
[20] P.R. Rhodes, E.P. Wolfarth, Proc. R. Soc. 273 (1963) 347.
[21] P. Deppe, M. Rosenberg, Solid State Commun. 64 (1987) 1247.
[22] O. Isnard, D. Fruchart, J. Alloys Compd. 205 (1994) 1.
[23] C. Chacon, O. Isnard, J. Appl. Phys. 89 (2001) 71–75.
[24] L. Gelato, J. Appl. Cryst. 14 (1981) 151–153.
[25] V. Paul-Boncour, S.M. Filipek, A. Percheron-Guegan, I. Marchuk, J. Pielaszek, J. Alloys Compd. 317–318 (2001) 83–87.
[26] V. Paul-Boncour, S. Matar, Phys. Rev. B 70 (2004) 184435.